



Statistical characterization of the effect of random core loss on the intercore crosstalk in long-haul uncoupled multicore fiber links

JOÃO L. REBOLA^{1,2,*}  AND ADOLFO V. T. CARTAXO^{1,2}

¹*Optical Communications and Photonics Group, Instituto de Telecomunicações, Lisbon, Portugal*

²*Instituto Universitário de Lisboa (Iscte-IUL), Lisbon, Portugal*

*joao.rebola@iscte-iul.pt

Abstract: We characterize the statistical properties of direct average intercore crosstalk (ICXT) in long-haul uncoupled multicore fiber (MCF) links consisting of concatenated MCF segments, where core dependent loss (CDL) in each segment varies randomly. Numerical simulation results show that the direct average ICXT power at the output of long-haul MCF links with random CDL is well described by a Gaussian distribution. A statistical distribution, which accounts for only two values of core loss (the highest and lowest core loss) with equal probability, is proposed as the worst-case distribution of core loss resulting in the maximum excess of direct average ICXT power. With this distribution, practical values of random CDL, 20 MCF segments per span and 2000 km-long links, analytical and simulation results show the maximum excess of direct average ICXT power does not exceed 0.25 dB, being further lower for a higher number of segments. An analytical approximation for the maximum excess of direct average ICXT power in long-haul uncoupled MCF links with similar spans is presented. Demonstrating high accuracy (with less than 0.02 dB discrepancy relative to simulation results in all cases evaluated), this approximation provides a simple and efficient means for estimating the worst-case impact of random CDL on ICXT power in long-haul MCF links.

© 2024 Optica Publishing Group under the terms of the [Optica Open Access Publishing Agreement](#)

1. Introduction

Space-division multiplexing with multicore fibers (MCFs) is seen as a future solution to cope with current capacity constraints in single-core singlemode fibers, lowering the cost per bit in telecommunication links where the available physical space is limited, such as submarine cables [1–3] or datacenter interconnects [3–5]. Even with uncoupled cores, the quality of signal transmission in MCFs may be degraded by intercore crosstalk (ICXT), especially in the case of unidirectional transmission [2,6,7]. The ICXT in uncoupled MCFs has been studied considering equal and fixed core losses [8–11]. However, due to manufacturing imperfections, uncoupled MCFs usually exhibit core dependent loss (CDL) [12–14]. The impact of CDL on the average power of direct ICXT (which occurs when signals in adjacent cores are transmitted in the same propagation direction) in two-core unsegmented uncoupled MCFs has been studied theoretically for unidirectional transmission [15,16] and bidirectional transmission [16]. For both kinds of transmission, the direct average ICXT power (hereafter referred to briefly as ICXT power) with fixed CDL along the span can vary 2 dB (for CDL between -0.04 and 0.04 dB/km) in comparison with MCFs with equal core losses [16]. The excess of ICXT power was introduced [17] to quantify the increase of average ICXT power induced by random CDL relative to its mean (case without CDL). In unidirectional links, for a uniformly distributed cores' loss with CDL range of 0.08 dB/km in each MCF segment, the excess of ICXT power at the output of 100 km span can reach about 1 dB [18], while it was shown that, it does not exceed 0.2 dB, for 2000 km-long links with multiple spans [17]. Evaluating the representativeness of this excess ICXT power figure and how it is influenced by the statistical distribution of cores' loss remains a task at hand.

This work extends the analysis presented in [17,18] by studying analytically and through numerical simulation the effect of random CDL on the statistical properties of the direct average ICXT power in long-haul uncoupled MCF optical links. The statistical distribution of cores' loss, shown to lead to the highest excess ICXT power under some conditions (worst-case distribution), is assessed analytically and tested numerically by comparison with two alternative distributions. Relying on the excess of ICXT power and the worst-case distribution, design considerations for long-haul uncoupled MCF links impaired by ICXT with random CDL are reported.

2. Numerical model for direct average ICXT power characterization

This section describes the numerical model used to study the statistical behavior of the average ICXT power in long-haul uncoupled MCF links. Without loss of generality and to simplify the description, a two-core fiber is considered. Each link consists of N_s optically amplified MCF spans, being the k -th span composed of N_k concatenated MCF segments (with N_k-1 splice points). The length of the i -th segment of the k -th span is $L_{i,k}$. Each span is terminated with a multicore-optical amplifier (MC-OA). The equivalent model of the k -th span (with $k = 1, \dots, N_s$) is depicted in Fig. 1, and follows closely the model presented in [18,19]. The total length of the k -th span is $L_{s,k} = \sum_{i=1}^{N_k} L_{i,k}$.

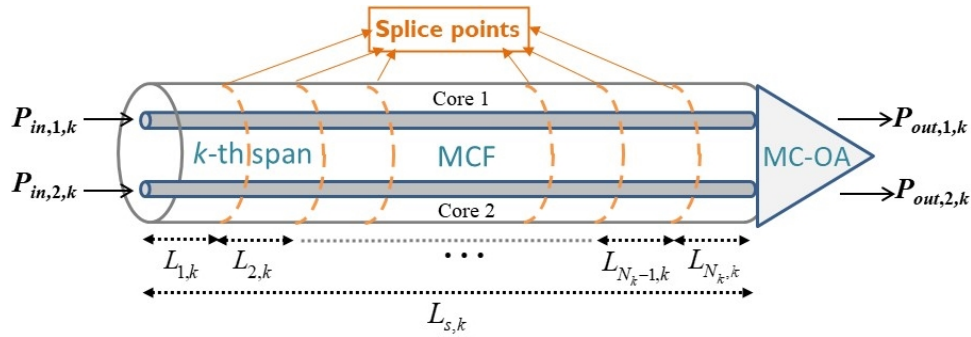


Fig. 1. Equivalent model of the k -th span, with N_k MCF segments in the span, N_k-1 splice points, considering a fiber with two cores and multicore optical amplification at the end of the fiber span.

The average power at the output of the k -th span, $P_{out,c,k}$ (with $c = 1$ for core 1 and $c = 2$ for core 2) is given by [15]

$$\begin{bmatrix} P_{out,1,k} \\ P_{out,2,k} \end{bmatrix} = \mathbf{T}_{OA,k} \mathbf{T}_{N_k,k} \mathbf{C}_{N_k-1,k} \mathbf{T}_{N_k-1,k} \cdots \mathbf{C}_{2,k} \mathbf{T}_{2,k} \mathbf{C}_{1,k} \mathbf{T}_{1,k} \begin{bmatrix} P_{in,1,k} \\ P_{in,2,k} \end{bmatrix} \quad (1)$$

where $P_{in,c,k}$ (with $c = 1$ or 2) stands for the average power at the input of the k -th span. Each matrix $\mathbf{T}_{i,k}$ (with $i = 1, \dots, N_k$ and $k = 1, \dots, N_s$) represents the coupled power equations with CDL between cores 1 and 2 in the i -th MCF segment of the k -th span in matricial form [15]. Each matrix $\mathbf{T}_{i,k}$ is given by [15,16]

$$\mathbf{T}_{i,k} = \exp[-(\bar{\alpha}_{i,k} + h_{i,k})L_{i,k}] \begin{bmatrix} \cosh(\eta_{i,k}L_{i,k}) - \delta_{\alpha,i,k}L_{i,k} \cdot \frac{\sinh(\eta_{i,k}L_{i,k})}{\eta_{i,k}L_{i,k}} & h_{i,k}L_{i,k} \frac{\sinh(\eta_{i,k}L_{i,k})}{\eta_{i,k}L_{i,k}} \\ h_{i,k}L_{i,k} \frac{\sinh(\eta_{i,k}L_{i,k})}{\eta_{i,k}L_{i,k}} & \cosh(\eta_{i,k}L_{i,k}) + \delta_{\alpha,i,k}L_{i,k} \cdot \frac{\sinh(\eta_{i,k}L_{i,k})}{\eta_{i,k}L_{i,k}} \end{bmatrix} \quad (2)$$

$$\eta_{i,k} = (h_{i,k}^2 + \delta_{\alpha,i,k}^2)^{1/2} \quad (3)$$

where $h_{i,k}$ is the power coupling coefficient between the two cores in the i -th segment of the k -th span; $\bar{\alpha}_{i,k}$ is the average of the loss coefficients of the two cores in the i -th segment of the k -th span and is given by $\bar{\alpha}_{i,k} = (\alpha_{1,i,k} + \alpha_{2,i,k})/2$, with $\alpha_{c,i,k}$ ($c = 1$ or 2) corresponding to the loss coefficient of core c in the i -th segment; and $\delta_{\alpha,i,k} = (\alpha_{1,i,k} - \alpha_{2,i,k})/2$. The loss coefficient imbalance (that corresponds to CDL) is given by $2\delta_{\alpha,i,k}$ [15].

Due to manufacturing imperfections, CDL values in the interval $[-0.04, 0.04]$ dB/km have been reported [14], and it is very unlikely that CDL exceeds 0.1 dB/km [15]. As the MCF segments can come from different lots, the cores' loss coefficients $\alpha_{1,i,k}$ and $\alpha_{2,i,k}$ can be (arbitrarily) different from segment to segment. Hence, the loss coefficients $\alpha_{1,i,k}$ and $\alpha_{2,i,k}$ of the i -th MCF segment of the k -th span may be characterized as random variables (RVs) and, consequently, the CDL of each segment is also a RV. So, each segment exhibits random CDL, which is considered to be independent of CDL of other segments.

By varying the coupling coefficient $h_{i,k}$ along the MCF segments and along the overall MCF link length, the ICXT power deviation, either due to manufacturing imperfections or to the influence of other neighboring cores, can also be included in the MCF link model.

In each splice point, the matrices $\mathbf{C}_{i,k}$ (with $i = 1, \dots, N_k - 1$ and $k = 1, \dots, N_s$) in Eq. (1) are defined by [19]

$$\mathbf{C}_{i,k} = \begin{bmatrix} \eta_{11,i,k} & \eta_{12,i,k} \\ \eta_{21,i,k} & \eta_{22,i,k} \end{bmatrix} \quad (4)$$

where $\eta_{cc,i,k}$ (with $c = 1$ or 2) defines the loss of the splice point for core c in the i -th segment of the k -th span and $\eta_{c'c',i,k}$ (with $c' \neq c$) defines the mode coupling between the two cores at the i -th splice point of the k -th span. The loss of each splice point can be set using the splice loss difference definition proposed in [19]. The matrices $\mathbf{C}_{i,k}$ in Eq. (4) can be approximated by diagonal matrices, since the ICXT caused by the mode coupling at the splice point is typically low when compared to the ICXT generated in the MCF [19].

After N_k MCF segments, an ideal MC-OA perfectly compensates the optical loss in each core. As the main goal of this work is to study the effect of random CDL on the average ICXT power, the noise of the amplifiers is not considered in the analysis performed. With perfect core loss compensation, the gain of the MC-OA in each core is equal to the overall loss of the k -th span, and the gain matrix $\mathbf{T}_{OA,k}$ used in (1) is given by

$$\mathbf{T}_{OA,k} = \begin{bmatrix} \exp\left(\sum_{i=1}^{N_k} \alpha_{1,i,k} L_{i,k}\right) & 0 \\ 0 & \exp\left(\sum_{i=1}^{N_k} \alpha_{2,i,k} L_{i,k}\right) \end{bmatrix}, \text{ with } k = 1, \dots, N_s \quad (5)$$

where it is assumed that the ICXT in the MC-OAs is negligible relative to the ICXT induced by the MCF, being $\mathbf{T}_{OA,k}$ a diagonal matrix.

At the output of the long-haul MCF link with a total length L_{tot} after N_s spans ($L_{tot} = \sum_{k=1}^{N_s} L_{s,k}$), the average optical power in each core (also denoted as forward propagating power [16]) is obtained by applying Eq. (1) from the first to the last span, and is given by

$$\begin{bmatrix} P_{out,1,N_s} \\ P_{out,2,N_s} \end{bmatrix} = \mathbf{T}_{OA,N_s} \mathbf{T}_{N_s,N_s} \mathbf{C}_{N_s-1,N_s} \cdots \mathbf{C}_{1,N_s} \mathbf{T}_{1,N_s} \cdots \mathbf{T}_{OA,1} \mathbf{T}_{N_1,1} \mathbf{C}_{N_1-1,1} \cdots \mathbf{C}_{1,1} \mathbf{T}_{1,1} \begin{bmatrix} P_{in,1,1} \\ P_{in,2,1} \end{bmatrix} \quad (6)$$

Equation (6) can also include the influence of the fan-in, fan-out on the output average optical power, by using the corresponding power transfer matrices presented in [15].

The direct average ICXT power, XT_{dir} , in core c (with $c = 1$ or 2) at the output of the long-haul MCF link is given by [16]

$$XT_{dir,c} = P_{cou,c}(L_{tot})/P_{sig,c}(L_{tot}) \quad (7)$$

where $P_{cou,c}(L_{tot})$ is the coupled power in core c at link output induced by the signal launched in the other core and $P_{sig,c}(L_{tot})$ is the signal power in core c at link output. The coupled power $P_{cou,c}(L_{tot})$ is obtained from $P_{out,c,Ns}$ as given by (6), by injecting power $P_{in,c',1}$ at the link input in the other core, c' , with $c' \neq c$. The signal power $P_{sig,c}(L_{tot})$ is obtained from $P_{out,c,Ns}$, by setting the power coupling coefficient, $h_{i,k}$, to zero [16] (the elements outside the main diagonal of each matrix $\mathbf{T}_{i,k}$ as defined in (2) become zero).

The MCF link model proposed in this work allows to study the influence of the statistics of the segment length $L_{i,k}$, the coupling coefficient, $h_{i,k}$, and the number of segments in each span, N_k , on the link output power and, consequently, on the ICXT power. However, as the main goal of this work is to statistically characterize the effect of random CDL on the ICXT power in long-haul MCF links, all segment and span parameters, with the exception of CDL, are constant and deterministic along the MCF link in the remainder of this work. Hence, the segment length is considered constant, $L_{i,k} = L$; the coupling coefficient is the same in the two cores, $h_{i,k} = h$; the number of segments in each span is equal, $N_k = N$; and the splice points are considered to have equal losses in the two cores along the MCF link.

In the following, the average of the direct ICXT power at the link output (given by (7)) obtained without CDL is called average ICXT level [8]. In most practical situations, the average ICXT level can be approximated by hL_{tot} [16].

3. Worst-case cores' loss distribution and derivation of the mean and standard deviation of the ICXT power

Equation (7) shows that, when the CDL of each segment is random, the ICXT power is random as well. It has been shown that, when the cores' loss of each segment follows a uniform distribution, the probability density function (PDF) of the ICXT power is nearly Gaussian-distributed for a sufficiently high number of MCF segments [17]. The Gaussian distribution is also expected for the ICXT power when the cores' loss follows other distributions (this subject is further discussed in section 5). Hence, in this situation, it is sufficient to evaluate the mean and standard deviation of the ICXT power to have a complete statistical description of its dependence on the random CDL.

With the final goal of deriving analytical expressions of the mean and standard deviation of the ICXT power, we start by obtaining a simplified closed form expression of the ICXT power resulting from one span with N MCF segments with arbitrary cores' loss coefficients. Perfect cores' loss compensation by MC-OAs is assumed. As only one span is considered, the index k concerning a specific k -th span will be dropped for notation simplification. The coupled power in core c (with $c \neq c'$) at the output of one span consisting of N MCF segments with random CDL, $P_{cou,c}$, results from the sum of N contributions with each contribution corresponding to a different segment. Focusing for now our attention on segment j , the power at the input of segment j in core c' , $P_{c',j}$, resulting from the random loss in core c' is given by

$$P_{c',j} = P_{in,c'} \exp \left[- \sum_{i=1}^{j-1} \alpha_{c',i} L \right] \quad (8)$$

where $P_{in,c'}$ is the average power in core c' at the span input. Also, for low coupled power (situation of practical interest), the power coupled from core c' to core c at segment j , $P_{h,j}$, can be

approximated by [15]

$$P_{h,j} = hL \exp \left[-\frac{\alpha_{c,j} + \alpha_{c',j}}{2} L \right] P_{c',j} \quad (9)$$

Consequently, the coupled power that propagates in core c from the input of segment $j+1$ (generated in segment j) to the output of the last segment, $P_{c,j}$, is given by

$$P_{c,j} = \exp \left[-\sum_{i=j+1}^N \alpha_{c,i} L \right] P_{h,j} \quad (10)$$

The total coupled power in core c at the output of the last segment resulting from the contributions of all segments of that span, $P_{cou,c}$, is obtained from (8)–(10) by summing all coupled power contributions of the N segments, $P_{cou,c} = \sum_{j=1}^N P_{c,j}$, and can be written as

$$P_{cou,c} = \sum_{j=1}^N P_{in,c} \exp \left[-\sum_{i=1}^{j-1} \alpha_{c',i} L \right] hL \exp \left[-\frac{\alpha_{c,j} + \alpha_{c',j}}{2} L \right] \exp \left[-\sum_{i=j+1}^N \alpha_{c,i} L \right] \quad (11)$$

The signal power in core c at the output of the last segment is affected by loss of core c and is given by

$$P_{sig,c} = P_{in,c} \exp \left[-\sum_{i=1}^N \alpha_{c,i} L \right] \quad (12)$$

where $P_{in,c}$ is the average power in core c at the span input. By substituting (11) and (12) in (7), considering the same average power in cores c and c' at the span input ($P_{in,c} = P_{in,c'}$), the ICXT power in core c at the output of a span with N MCF segments can be written as

$$XT_{dir,c} = \sum_{j=1}^N hL \exp \left[-L \left(\sum_{i=1}^{j-1} \alpha_{c',i} - \sum_{i=1}^{j-1} \alpha_{c,i} + \frac{\alpha_{c',j} - \alpha_{c,j}}{2} \right) \right] \quad (13)$$

With perfect loss compensation in each span, Eq. (13) is the contribution of the ICXT power of the considered span to the overall ICXT power at the link output because both coupled and signal powers at the span output are transmitted to the link output with the same gain. As a consequence, the overall ICXT power at the link output is the sum of N_s terms, each one resulting from a different span and formally given by Eq. (13) but with different values of the cores' loss, resulting from the random cores' loss. It was confirmed that, for ICXT power lower than -10 dB, Eq. (13) provides estimates of the ICXT power in very good agreement with the figures of the ICXT power obtained using the numerical model presented in section 2.

The study of the dependence of the ICXT power on the core loss imbalance presented in [16] for fixed core's loss shows that, as higher the core loss imbalance is, higher is the increase of ICXT power relative to core loss balanced case. Apparently, this means that, in case of random cores' loss, the ICXT power will be higher when the cores' loss occurrence concentrates in specific (higher) values. However, the randomness of loss from segment to segment along the span may mitigate the effect of core loss on the ICXT power observed in cases of higher loss imbalance with fixed core loss. To analytically evaluate the influence of loss randomness from segment to segment on ICXT power, understanding the PDF for the cores' loss is crucial. As of the authors' knowledge, the PDF for the cores' loss remains unknown. Hence, a worst-case CDL distribution is targeted to facilitate the assessment of the most severe performance degradation resulting from random CDL. To this end, the cores' loss occurrence in each segment is clustered in specific values constrained to the same core loss mean (which, in case of absence of core loss imbalance, is equal to the core loss for all segments) and to the range of core loss (between $\alpha_{c,min}$

and $\alpha_{c,max}$). We begin by considering the occurrence of only two values of core loss which are equally probable (this assumption is revisited in the last paragraph in this section). In this case, the PDF of each one of $\alpha_{c,i}$ and $\alpha_{c',i}$ ($1 \leq i \leq N$) in Eq. (13) is given by

$$p(y) = \frac{1}{2}\delta(y - \langle\alpha\rangle - x) + \frac{1}{2}\delta(y - \langle\alpha\rangle + x) \quad (14)$$

where $\delta(y)$ stands for the Dirac delta function, $\langle\alpha\rangle$ is the cores' loss mean (the same for both cores) and x determines the two possible values the cores' loss may take on. For core loss between $\alpha_{c,min}$ and $\alpha_{c,max}$, $\langle\alpha\rangle = (\alpha_{c,min} + \alpha_{c,max})/2$, and x may be between 0 and $x_{max} = (\alpha_{c,max} - \alpha_{c,min})/2$. Our purpose is to find the value of x that maximizes the excess ICXT power because that value provides information on the PDF which corresponds to the worst ICXT performance induced by random CDL (worst-case distribution).

The mean of the ICXT power at the output of one span with N MCF segments can be computed using (13) and (14). After algebraic manipulation, the mean can be written as

$$\mu_1 = E[XT_{dir,c}] = hL \cosh^2\left(\frac{1}{2}Lx\right) \cdot \frac{[\cosh^2(Lx)]^N - 1}{\cosh^2(Lx) - 1} \quad (15)$$

where $E[Z]$ is the expected value of Z . We notice that, for the cases of CDL with practical interest, the approximation $|L \cdot x| \ll 1$ is valid. In this case, the mean can be approximated by $\mu_1 \approx NhL$, which is the result obtained in the absence of CDL [15,16].

Similarly, using (13) and (14), the mean-square value of the ICXT power at the output of one span with N MCF segments can be written as

$$E[XT_{dir,c}^2] = \left\{ \left[\cosh^2(Lx) - \frac{2\cosh^2\left(\frac{3}{2}Lx\right)\cosh^2\left(\frac{1}{2}Lx\right)}{\cosh^2(Lx) - 1} \right] \cdot \frac{[\cosh^2(2Lx)]^N - 1}{\cosh^2(2Lx) - 1} + \frac{2\cosh^2\left(\frac{3}{2}Lx\right)\cosh^2\left(\frac{1}{2}Lx\right)}{\cosh^2(Lx) - 1} \cdot \frac{[\cosh^2(2Lx)]^N - [\cosh^2(Lx)]^N}{\cosh^2(2Lx) - \cosh^2(Lx)} \right\} \cdot (hL)^2 \quad (16)$$

An expression of the standard deviation of the ICXT power at the output of one span, σ_1 , can be obtained using $\sigma_1 = (E[XT_{dir,c}^2] - \mu_1^2)^{1/2}$, where μ_1 and $E[XT_{dir,c}^2]$ are given by Eqs. (15) and (16), respectively. For $|L \cdot x| \ll 1$, the standard deviation at the output of one MCF span is well approximated by

$$\sigma_1 \approx \sqrt{\frac{2N^3}{3}} h x L^2 \quad (17)$$

For links with N_s independent spans and the same PDF of core loss in all segments, the ICXT power generated in each span is uncorrelated to the ICXT power generated in other segments, and the mean and standard deviation are given by $\mu_{N_s} = N_s \mu_1$ and $\sigma_{N_s} = N_s^{1/2} \sigma_1$, respectively. As the excess ICXT power increases with the ratio σ_{N_s} / μ_{N_s} [17], which means it increases with σ_1 / μ_1 for similar and independent spans, Eqs. (15) and (16) show that, for CDL of interest, the highest value of excess ICXT power happens for the maximum value of x . If the core loss is distributed by more than two values, then others than the maximum value of x occur and a lower standard deviation is obtained. In this case, the corresponding PDF leads to a lower excess ICXT power than the one corresponding to Eqs. (15) and (16). For a continuous PDF, where the core loss is distributed across a continuum of values, each contributing less to the standard deviation than when x assumes its maximum value only, we expect a lower excess ICXT power compared to what is indicated by Eqs. (15) and (16). Hence, setting x to its maximum value, x_{max} , in Eq. (14),

the worst-case distribution of core loss is given by

$$p(y) = \frac{1}{2}\delta(y - \alpha_{c,min}) + \frac{1}{2}\delta(y - \alpha_{c,max}) \quad (18)$$

and is designated hereafter as “equally probable edges” (EPE) distribution. With the EPE distribution, Eq. (17) can be written

$$\sigma_{1,max} \approx \sqrt{\frac{N^3}{6}}h(\alpha_{c,max} - \alpha_{c,min})L^2 \quad (19)$$

The accuracy of Eq. (17) is discussed in sections 5 and 6.

To test the validity of the assertions of the preceding paragraph, in Section 5, we compare the ICXT power acquired through modeling random core loss with two continuous PDFs against the ICXT power obtained using the EPE distribution.

4. Random CDL effect on the ICXT power for the EPE distribution

In this section, the statistical dependence of the ICXT power on random CDL in long-haul uncoupled MCF links is assessed using Monte Carlo simulation and the model presented in Section 2. In each realization of the Monte Carlo simulation, the EPE distribution is used to generate independently the loss coefficients $\alpha_{c,i}$ of all segments.

Unless otherwise stated, all results presented in this work are obtained for a power $P_{in,1,1} = P_{in,2,1} = 1$ mW at the input of the MCF link, considering the total link length of $L_{tot} = 2000$ km ($N_s = 20$ and $L_s = 100$ km). Each span has $N = 50$ segments with equal length $L = 2$ km. The attenuation coefficients $\alpha_{c,i}$ are generated within the interval [0.15, 0.23] dB/km, being the maximum core loss imbalance $2\delta_{\alpha,max} = 0.08$ dB/km.

Figure 2 shows the PDFs of the ICXT power at the output of the a) first span (100 km), b) middle span (1000 km) and c) last span (2000 km), for $h = 5 \times 10^{-10}$ m⁻¹. In this case, after 100 km, 1000 km and 2000 km, the average ICXT level is, respectively, $hL_{tot} = 5 \times 10^{-5}$ (−43 dB), 5×10^{-4} (−33 dB) and 1×10^{-3} (−30 dB). The latter corresponds to the average ICXT level that must be met to maximize the spectral efficiency in uncoupled MCF repeated coherent systems with span lengths of around 100 km [2]. Gaussian PDFs with the same mean, μ , and standard deviation, σ , as the ones obtained by simulation are also shown. The PDFs are estimated with 10^6 Monte Carlo realizations of the long-haul MCF link. In each realization, the MCF segments have different loss coefficients. As shown in Fig. 2, the Gaussianity of the PDFs of the ICXT power, XT_{dir} , is more pronounced for long-haul links (2000 km) than for shorter links (100 km) due to the higher number of concatenated MCF segments with random CDL (1000 against 50).

To quantify how an estimated PDF is close to the Gaussian shape, the excess kurtosis κ_E is used [20]. As a reference, a Gaussian PDF has null excess kurtosis. After 100 km, the excess kurtosis is $\kappa_E = 0.229$ and the PDF in Fig. 2(a) shows a more deviated Gaussian behavior than the PDF shown in Fig. 2(b) obtained after 1000 km, where $\kappa_E = 0.0193$. The Gaussian behavior becomes even more enhanced for longer distances, with $\kappa_E = 0.0189$ after 2000 km. For other link lengths, we have also observed an enhanced PDFs Gaussian behavior with the increase of the link length. As reported in [17,18], the PDFs become more Gaussian with the increase of the number of segments. As the number of random contributions to the total ICXT power (with each contribution coming from a different segment) increases with the number of segments, the PDF tends to approach a Gaussian distribution by the central limit theorem. As a consequence, the level of Gaussianity does not depend on the specific value of L , h and L_{tot} , but only on the number of segments.

This last conclusion can be confirmed in the numerical results shown in Table 1, where the mean, standard deviation and excess kurtosis of the ICXT power after 100 km, 1000 km and 2000 km obtained numerically using the EPE distribution for core loss are presented and the

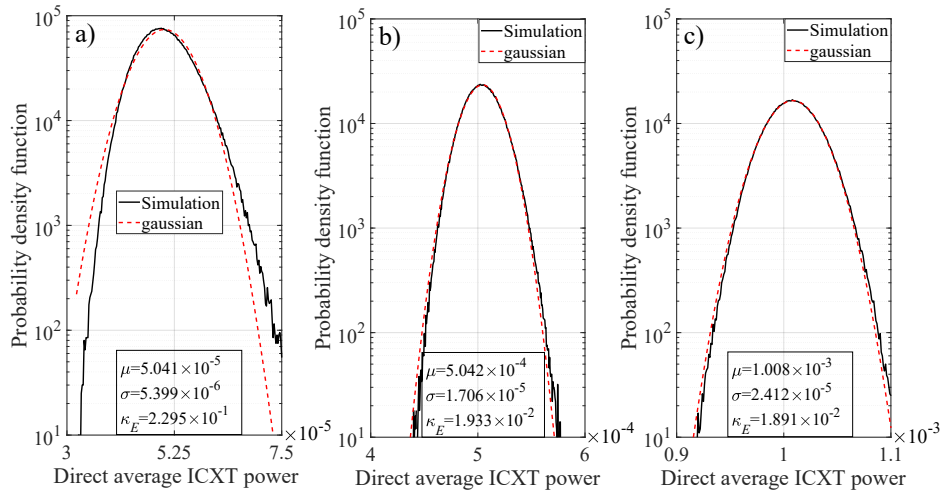


Fig. 2. PDFs of the ICXT power, after the a) first span (100 km), b) middle span (1000 km) and c) last span (2000 km), for $h = 5 \times 10^{-10} \text{ m}^{-1}$ with the EPE distribution for the core loss. The Gaussian PDFs shown are obtained with the mean μ and standard deviation σ estimated by simulation. The excess kurtosis κ_E is also shown.

coupling coefficient is varied. In Table 1, for all coupling coefficients (or average ICXT level at the link output after 2000 km), the excess kurtosis is below 3×10^{-2} after 1000 km (500 concatenated segments) indicating a higher level of Gaussianity than the one obtained after 100 km (50 concatenated segments). The level of Gaussianity is further improved after 2000 km (1000 concatenated segments), as the excess kurtosis is even lower. Hence, as long as the number of segments is sufficiently high, we can conclude that, due to the high level of Gaussianity, it is only sufficient to assess the mean and standard deviation of the ICXT power to have a good description of its statistical dependence with the EPE distribution for core loss.

Table 1. Mean, standard deviation and excess kurtosis of the ICXT power obtained by numerical simulation, for link lengths of 100, 1000 and 2000 km, and coupling coefficients of $h = 5 \times 10^{-11} \text{ m}^{-1}$, $5 \times 10^{-10} \text{ m}^{-1}$, $5 \times 10^{-9} \text{ m}^{-1}$ and $5 \times 10^{-8} \text{ m}^{-1}$. These coupling coefficients correspond to the average ICXT levels after 2000 km of $hL_{tot} = -40 \text{ dB}$, -30 dB , -20 dB and -10 dB , respectively

μ	$hL_{tot} = -40\text{dB}$	$hL_{tot} = -30\text{dB}$	$hL_{tot} = -20\text{dB}$	$hL_{tot} = -10\text{dB}$
100 km	5.042×10^{-6}	5.041×10^{-5}	5.042×10^{-4}	5.042×10^{-3}
1000 km	5.042×10^{-5}	5.042×10^{-4}	5.042×10^{-3}	5.044×10^{-2}
2000 km	1.008×10^{-4}	1.008×10^{-3}	1.009×10^{-2}	1.010×10^{-1}
σ	$hL_{tot} = -40\text{dB}$	$hL_{tot} = -30\text{dB}$	$hL_{tot} = -20\text{dB}$	$hL_{tot} = -10\text{dB}$
100 km	5.394×10^{-7}	5.399×10^{-6}	5.398×10^{-5}	5.392×10^{-4}
1000 km	1.707×10^{-6}	1.706×10^{-5}	1.706×10^{-4}	1.706×10^{-3}
2000 km	2.413×10^{-6}	2.412×10^{-5}	2.410×10^{-4}	2.416×10^{-3}
κ_E	$hL_{tot} = -40\text{dB}$	$hL_{tot} = -30\text{dB}$	$hL_{tot} = -20\text{dB}$	$hL_{tot} = -10\text{dB}$
100 km	2.273×10^{-1}	2.295×10^{-1}	2.336×10^{-1}	2.176×10^{-1}
1000 km	1.467×10^{-2}	1.933×10^{-2}	2.256×10^{-2}	2.749×10^{-2}
2000 km	3.436×10^{-3}	1.891×10^{-2}	1.224×10^{-2}	1.675×10^{-2}

Figure 2 and Table 1 show also that the mean of the ICXT power is approximately given by hL_{tot} meaning that, for random core loss, the mean is practically independent of CDL [17], even for pessimistic average ICXT levels. For a specific link length, the standard deviation grows linearly with the increase of the average ICXT level after 2000 km, hL_{tot} . Table 1 indicates also that, for the same average ICXT level, the standard deviation increases with the square root of the link length. These simulation findings agree with the discussion presented in Section 3.

With the EPE distribution for loss coefficients, the PDF of the ICXT power at the link output follows closely a Gaussian distribution, as it happens also when the uniform distribution is considered for random CDL [17,18]. The standard deviation and excess kurtosis shown in Table 1 for $hL_{tot} = -10$ dB, are higher than the ones shown in Fig. 1 of [17], which has been obtained by using the uniform distribution for random core loss and considering the same simulation parameters used to obtain Table 1. This indicates that the random CDL has a stronger impact on the ICXT power, leading to less Gaussian PDFs when the EPE distribution is used for the loss coefficients, instead of the uniform distribution. As the PDF obtained with the EPE distribution is less Gaussian, a higher number of segments will be required to approach the same level of Gaussianity obtained with the uniform distribution. In section 5, this subject is further studied and discussed.

5. Random CDL effect on the ICXT power considering different statistical distributions

In this section, we study the impact of considering different statistical distributions for the loss coefficient on the statistical properties of the ICXT power. The numerical results of this section are obtained with the power coupling coefficient of $h = 5 \times 10^{-10} \text{ m}^{-1}$. The values of other parameters of the long-haul uncoupled MCF link are equal to the ones considered in section 4.

Three different statistical distributions are considered for the loss coefficients $\alpha_{c,i}$ along the interval $[\alpha_{c,min}, \alpha_{c,max}]$: EPE, uniform and arcsine distributions. In the uniform distribution, the loss coefficients $\alpha_{1,i}$ and $\alpha_{2,i}$ in the i -th MCF segment can assume any value within the range $[\alpha_{c,min}, \alpha_{c,max}]$ with equal probability. The corresponding PDF is given by

$$p(y) = \begin{cases} \frac{1}{\alpha_{c,max} - \alpha_{c,min}}, & \text{for } \alpha_{c,min} \leq y \leq \alpha_{c,max} \\ 0, & \text{otherwise} \end{cases} \quad (20)$$

With the arcsine distribution, the loss coefficients $\alpha_{1,i}$ and $\alpha_{2,i}$ in the i -th MCF segment can assume any value within the range $[\alpha_{c,min}, \alpha_{c,max}]$, with the values closer to the interval edges having a higher probability. From the results and discussion presented in Section 3, this distribution is expected to lead to a higher impact of the CDL effect on the ICXT power relative to the impact with the uniform distribution, as values of core loss close to the interval edges are more likely to occur. The arcsine PDF is given by [21]

$$p(y) = \frac{1}{\pi \sqrt{(y - \alpha_{c,min})(\alpha_{c,max} - y)}}, \text{ for } \alpha_{c,min} \leq y \leq \alpha_{c,max} \quad (21)$$

It should be emphasized that the probability of occurrence of higher loss coefficient imbalance increases when “we move” from PDF given by Eq. (20) to PDF given by Eq. (21) and even further when “we move” to PDF given by Eq. (14).

Figure 3(a) and (b) show, respectively, the standard deviation σ and excess kurtosis κ_E of the ICXT power as a function of long-haul uncoupled MCF link length, when using the EPE, arcsine and uniform distributions for the loss coefficients in each MCF segment. For each distribution, 10^7 Monte Carlo realizations of the long-haul MCF link are required to obtain more stabilized values of the excess kurtosis.

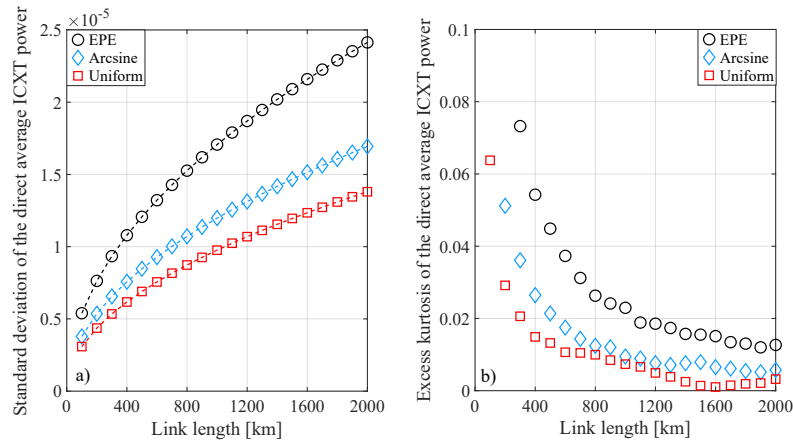


Fig. 3. a) Standard deviation σ and b) excess kurtosis κ_E of the ICXT power as a function of the MCF link length, for $h = 5 \times 10^{-10} \text{ m}^{-1}$, for the three statistical distributions used for the random core loss. In a), the symbols represent the results obtained using the numerical model described in Section 2, and the dashed lines correspond to results obtained by multiplying the value of the standard deviation obtained numerically after one span by $(N_s)^{1/2}$.

The mean μ of the ICXT power is not shown in Fig. 3, since it follows a linear growth with the link length, and its variation is practically the same for the three distributions. After one span (100 km), the mean obtained numerically with the model described in Section 2 and analytically using Eq. (15) is 5.0423×10^{-5} and 5.0422×10^{-5} , respectively. This very good agreement demonstrates the accuracy of the analytical expression of the mean of the ICXT power after one span given by Eq. (15) and that may be approximated by hL_s [15,17].

The numerical results (symbols) presented in Fig. 3(a) show that the standard deviation of the ICXT power grows with the increase of the link length, proportionally to $(N_s)^{1/2}$, as evidenced by the dashed lines in Fig. 3(a). These lines have been obtained by multiplying the numerical value of the standard deviation obtained after one span by $(N_s)^{1/2}$, for all the three distributions. After one span (100 km), the standard deviation obtained numerically with the EPE distribution, presented in Fig. 3(a), is $\sigma_1 = 5.3960 \times 10^{-6}$ and the standard deviation obtained analytically using Eqs. (15) and (16) is $\sigma_1 = 5.3955 \times 10^{-6}$. This very good agreement evidences the correctness of the analytical expression of the mean-square value of the ICXT power after one span given by Eq. (16). Using the approximation given by Eq. (17), the calculated standard deviation after one span is $\sigma_1 = 5.3174 \times 10^{-6}$, which corresponds to an error of 1.45% relative to the standard deviation obtained analytically using Eqs. (15) and (16). This small error shows the good accuracy of the approximation given by Eq. (17).

Figure 3(a) illustrates that the increase in the standard deviation is more pronounced for the EPE distribution. The standard deviation obtained with the uniform distribution shows the smaller increase with the link length, while the arcsine distribution leads to an intermediate increase. These results show that the EPE distribution leads to an enhanced impact of random CDL on the ICXT power. These numerical findings evidence that the EPE distribution yields the highest standard deviation of the ICXT power, supporting the validity of the claims made in Section 3 regarding the worst-case distribution of random core loss.

Figure 3(b) shows that the excess kurtosis approaches zero as the link length increases, meaning that the PDFs tend to be Gaussian for longer link lengths, due to the much higher number of concatenated MCF segments. For the EPE distribution, the excess kurtosis is above 0.01 at the output of the 2000 km-long MCF link (1000 concatenated MCF segments). For the other

two distributions, the excess kurtosis remains below 0.01 at roughly half the total link length, meaning that the random core loss with the EPE distribution reduces the level of Gaussianity of the ICXT power in comparison with the two other distributions.

6. Design considerations regarding the effect of random CDL on the ICXT power

The excess of the ICXT power can be used to quantify the increase of the ICXT power caused by CDL relative to the ICXT power obtained when CDL is null. The excess of the ICXT power, ΔXT_{dir} , is defined, in dB, as

$$\Delta XT_{dir}[\text{dB}] = 10 \log_{10} \left(\frac{XT_{dir,with\ CDL}}{XT_{dir,without\ CDL}} \right) \quad (22)$$

Without random CDL, the ICXT power is given by the mean μ . So, it can be shown that the excess of the ICXT power (with XT_{dir} in the range $[\mu - k\sigma, \mu + k\sigma]$) induced by CDL relative to the case without CDL is maximized by [17]

$$\Delta XT_{dir}[\text{dB}] = 10 \log_{10}(1 + k\sigma/\mu) \quad (23)$$

where k sets the range of variation of XT_{dir} . Considering $k = 3$ in Eq. (23) (corresponding to the 3σ rule of thumb), nearly all realizations of the long-haul MCF link (99.7%) have ICXT power in the range $[\mu - 3\sigma, \mu + 3\sigma]$, and half of them will lead to $\Delta XT_{dir} \geq 0$ dB. From (23), e.g., to keep the excess of ICXT power below 0.5 dB, the relative spread σ/μ should not exceed 4.07×10^{-2} .

From the results presented in section 5, it can be concluded that, for links with similar transmission features particularly random CDL, the relative spread at the output of the long-haul uncoupled MCF link only depends on the relative spread at the output of the first span, σ_1/μ_1 , that can be calculated analytically using (15) and (16), and on the number of spans. Hence, the excess of the ICXT power at the output of a MCF link with N_s spans with similar transmission features can be written as

$$\Delta XT_{dir}[\text{dB}] = 10 \log_{10} \left(1 + k \frac{1}{\sqrt{N_s}} \cdot \frac{\sigma_1}{\mu_1} \right) \quad (24)$$

By substituting Eq. (17) in (24), an approximation for the maximum excess of the ICXT power can be written as

$$\Delta XT_{dir,max}[\text{dB}] = 10 \log_{10} \left(1 + k \sqrt{\frac{L_s}{6L_{tot}}} \cdot \frac{1}{N} \cdot (\alpha_{c,max} - \alpha_{c,min}) L_s \right) \quad (25)$$

As (15) and (16) have been derived considering the EPE distribution, which is a worst-case distribution for random core loss, Eq. (25) can be viewed as the maximum excess of the ICXT power at the output of a MCF link with N_s similar spans. Notice that, to obtain this maximum value, only the number of segments, span length, link length and maximum and minimum core loss must be known. For a given link length, the maximum excess ICXT power given Eq. (25) varies with $N^{-1/2}$ and $L_s^{3/2}$. Hence, increasing the number of segments (shorter segments) and increasing the number of spans (shorter spans) reduces the excess of the ICXT power, decreasing the impact of random CDL on the ICXT power.

Figure 4 shows the excess of ICXT power as a function of the number of segments and half the maximum loss coefficient imbalance, considering $L_{s,k} = 100$ km, $L_{tot} = 2000$ km ($N_s = 20$) and $k = 3$. The loss coefficients of each segment take the values, $\alpha_{c,min} = 0.15$ dB/km and $\alpha_{c,max} = \alpha_{c,min} + 2\delta_{\alpha,max}$, with the range $\delta_{\alpha,max}$ varying as in Fig. 4. Notice that the relative spread is independent of the average ICXT level [17]; hence, the results shown in Fig. 4 are independent of the coupling coefficient, h . Figure 4(a) corresponds to results calculated with (23)

using the relative spread σ/μ at the link output obtained numerically. For each pair $(N, \delta_{\alpha, max})$, 10^6 Monte Carlo realizations of the long-haul MCF link have been simulated. Figure 4(b) presents analytical results obtained using the approximation (25). 99 pairs $(N, \delta_{\alpha, max})$ have been considered in Fig. 4. The very good agreement between the results shown in Fig. 4(a) and (b) evidences the good accuracy of (25) for estimating the excess of ICXT power. The highest difference found in Fig. 4 between numerical and analytical results is 0.01 dB. We obtained similar results to the ones presented in Fig. 4, for a different number of spans, and we have found that the highest difference of the excess of ICXT power estimated numerically and analytically with (25) is obtained for $N_s = 1$ and is 0.02 dB. This highest difference occurs for $\delta_{\alpha, max} = 0.04$ dB/km and $N = 20$. Figure 4 confirms that, to reduce the excess of ICXT power for a given CDL, it is preferable to have a higher number of segments (shorter segments) in each MCF span.

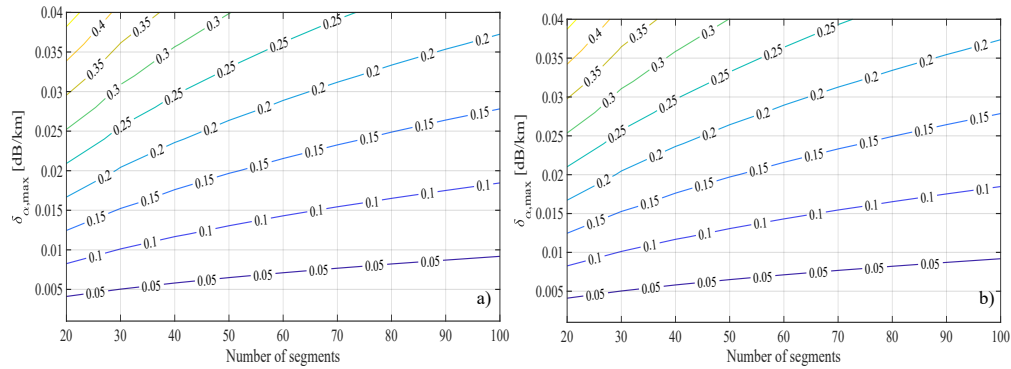


Fig. 4. Maximum excess of ICXT power, $\Delta XT_{dir,max}$, as a function of the number of segments and half the maximum loss coefficient imbalance $\delta_{\alpha,max}$, considering $L_{s,k} = 100$ km, $L_{tot} = 2000$ km ($N_s = 20$ spans) and $k = 3$. a) Numerical results; b) analytical results obtained using the approximation given by (25).

Figure 4 shows that, for $k = 3$ and $\delta_{\alpha,max} = 0.02$ dB/km, that corresponds to the maximum CDL value reported [14], the maximum excess of ICXT power decreases from 0.25 dB to 0.12 dB, when the number of segments increases from 20 to 100 (in this case, the relative spread at the output of one span varies between about 0.08 and 0.04).

7. Conclusion

This work has studied the effect of random CDL on the direct average ICXT power in long-haul uncoupled MCF links composed of concatenated MCF segments. Based on analytical expressions for the mean and standard deviation of ICXT power, a rationale has been provided to demonstrate that the EPE distribution represents a worst-case scenario for random core loss. Numerical simulations have corroborated this, showing a heightened impact of random core loss on ICXT power when employing the EPE distribution compared to uniform and arcsine distributions. Additionally, simulation results indicate that with the EPE distribution, the PDF of ICXT power closely resembles a Gaussian distribution for links consisting of a sufficiently high number of concatenated MCF segments.

Using the EPE distribution for the core loss, an analytical formulation has been presented to determine the maximum excess of ICXT power due to random CDL for MCF links with similar spans. Analytical and simulation results have shown that, for practical CDL values, the maximum excess of ICXT power due to random CDL relative to its mean varies between 0.12 and 0.25 dB, for 2000 km-long MCF links, depending on the number of MCF segments.

An analytical approximation for the maximum excess of ICXT power has also been introduced. With its high accuracy (less than a 0.02 dB discrepancy relative to simulation results in all cases evaluated), this approximation serves as a straightforward and efficient method for estimating the worst-case influence of random CDL on ICXT power in long-haul MCF links.

Funding. Fundação para a Ciência e a Tecnologia.

Acknowledgments. This work was supported in part by Fundação para a Ciência e Tecnologia/Ministério da Ciência, Tecnologia e Ensino Superior (FCT/MCTES) under Project UIDB/50008/2020.

Disclosures. The authors declare no conflicts of interest.

Data availability. Data underlying the results presented in this paper are not publicly available at this time but may be obtained from the authors upon reasonable request.

References

1. J. Downie, Y. Jung, S. Makovejs, *et al.*, “Cable capacity and cost/bit modeling of submarine MCF systems with MC-EDFA alternatives,” *J. Lightwave Technol.* **41**(11), 3559–3566 (2023).
2. T. Hayashi, T. Nagashima, A. Inoue, *et al.*, “Uncoupled multi-core fiber design for practical bidirectional optical communications,” in *Proc. of Opt. Fiber Commun. Conf. Exhib.* (2022), paper M1E.1.
3. T. Matsui, Y. Sagae, Y. Yamada, *et al.*, “High figure-of-merit multi-core fiber with standard cladding diameter for long-haul and wide-band transmission,” accepted for publication in *J. Lightwave Technol.*
4. L. Zhang, J. Chen, E. Agrell, *et al.*, “Enabling technologies for optical data center networks: spatial division multiplexing,” *J. Lightwave Technol.* **38**(1), 18–30 (2020).
5. R. Luís, B. Puttnam, G. Rademacher, *et al.*, “Multicore fiber interconnects for multi-terabit spine-leaf datacenter network topologies,” *J. Opt. Commun. Netw.* **15**(7), C41–C47 (2023).
6. T. Hayashi, “Accuracy of analytical expressions for Rayleigh backscattered crosstalk in bidirectional multi-core fiber transmissions,” *Opt. Express* **30**(13), 23943–23952 (2022).
7. M. Koshihara, Y. Kokubun, M. Nakagawa, *et al.*, “Behavior of intercore crosstalk in square-layout uncoupled four-core fibers,” *IEICE Electron. Express* **19**(18), 19.2022037920220379 (2022).
8. B. Pinheiro, J. Rebola, and A. Cartaxo, “Analysis of inter-core crosstalk in weakly-coupled multi-core fiber coherent systems,” *J. Lightwave Technol.* **39**(1), 42–54 (2021).
9. B. Puttnam, R. Luís, T. Eriksson, *et al.*, “Impact of intercore crosstalk on the transmission distance of QAM formats in multicore fibers,” *IEEE Photonics J.* **8**(2), 1–9 (2016).
10. T. Hayashi, T. Sasaki, E. Sasaoka, *et al.*, “Physical interpretation of intercore crosstalk in multicore fiber: effects of macrobend, structure fluctuation, and microbend,” *Opt. Express* **21**(5), 5401–5412 (2013).
11. A. Cartaxo and J. Morgado, “New expression for evaluating the mean crosstalk power in weakly-coupled multi-core fibers,” *J. Lightwave Technol.* **39**(6), 1830–1842 (2021).
12. Y. Tamura, T. Hayashi, T. Nakanishi, *et al.*, “Low-loss uncoupled two-core fiber for power efficient practical submarine transmission,” in *Proc. Opt. Fiber Commun. Conf. Exhib.* (2019), paper M1E.5.
13. D. Soma, S. Beppu, Y. Wakayama, *et al.*, “Trans-pacific class transmission over a standard cladding ultralow-loss 4-core fiber,” *Opt. Express* **30**(6), 9482–9493 (2022).
14. T. Matsui, T. Kobayashi, H. Kawakara, *et al.*, “118.5 Tbit/s transmission over 316 km-long multi-core fiber with standard cladding diameter,” in *Proc. OptoElectron. Commun. Conf. and Photonics Global Conf.* (2017).
15. Y. Kobayashi and T. Hayashi, “Behavior and measurement method of inter-core crosstalk in multicore fibers with core-dependent loss,” *Opt. Express* **31**(1), 502–508 (2023).
16. A. Cartaxo, “Loss imbalance effect on inter-core crosstalk in bidirectional uncoupled multi-core fiber transmission,” *J. Lightwave Technol.* **41**(18), 5911–5921 (2023).
17. J. Rebola and A. Cartaxo, “Statistical dependence of average intercore crosstalk on random loss in long-haul uncoupled MCF links,” in *Proc. of IEEE Photon. Conf.* (2023), paper TuC3.4.
18. J. Rebola and A. Cartaxo, “Effect of core-dependent loss on the intercore crosstalk in multicore fiber systems with concatenated random loss fiber segments,” in *Proc. Int. Conf. Transp. Opt. Netw.* (2023), paper Mo.C2.2.
19. A. Nakamura, T. Oda, and Y. Koshihiya, “Test method of splice points for constructing uncoupled multi-core fiber transmission line,” *J. Lightwave Technol.* **42**(5), 1616–1625 (2024).
20. A. Mood, F. Graybill, and D. Boes, *Introduction to the Theory of Statistics* (McGraw-Hill, 1974) Chap. 2.
21. I. Monroy and E. Tangdiongga, *Crosstalk in WDM Communication Networks* (Kluwer Academic Publishers, 2002), Chap. 5.